THE JOURNAL OF BIOLOGICAL CHEMISTRY
Vol. 276, No. 28, Issue of July 13, pp. 25783–25790, 2001

Printed in U.S.A.

Molecular Basis for the Homophilic Activated Leukocyte Cell Adhesion Molecule (ALCAM)-ALCAM Interaction*

Received for publication, December 14, 2000, and in revised form, April 12, 2001
Published, JBC Papers in Press, April 16, 2001, DOI 10.1074/jbc.M011272200

Léon C. L. T. van Kempen‡§, Judith M. D. T. Nelissen§¶, Winfried G. J. Degen‡, Ruurd Torensma¶, Ulrich H. Weidle‖, Henri P. J. Bloemers‡, Carl G. Figdor¶, and Guido W. M. Swart‡

From the ‡University of Nijmegen, Department of Biochemistry, P. O. Box 9101, NL-6500 HB Nijmegen, The Netherlands, the ¶Department of Tumor Immunology, University Medical Center St. Radboud, Nijmegen, The Netherlands, and ‖Roche Diagnostics GmbH, Nonnenwald 2, D-82372 Penzberg, Germany

Activated leukocyte cell adhesion molecule (ALCAM/CD166), a member of the immunoglobulin superfamily with five extracellular immunoglobulin-like domains, facilitates heterophilic (ALCAM-CD6) and homophilic (ALCAM-ALCAM) cell-cell interactions. While expressed in a wide variety of tissues and cells, ALCAM is restricted to subsets of cells usually involved in dynamic growth and/or migration processes. A structure-function analysis, using two monoclonal anti-ALCAM antibodies and a series of amino-terminally deleted ALCAM constructs, revealed that homophilic cell adhesion depended on ligand binding mediated by the membrane-distal amino-terminal immunoglobulin domain and on avidity controlled by ALCAM clustering at the cell surface involving membrane-proximal immunoglobulin domains. Co-expression of a transmembrane ALCAM deletion mutant, which lacks the ligand binding domain, and endogenous wild-type ALCAM inhibited homophilic cell-cell interactions by interference with ALCAM avidity, while homophilic, soluble ligand binding remained unaltered. The extracellular structures of ALCAM thus provide two structurally and functionally distinguishable modules, one involved in ligand binding and the other in avidity. Functionality of both modules is required for stable homophilic ALCAM-ALCAM cell-cell adhesion.

Adhesion molecules play an important role in development, leukocyte function, and homeostasis in multicellular organisms, which are mainly governed by inter- and intracellular communication via cell-cell interactions. Alterations in cellular adhesion and communication can contribute to uncontrolled cell growth (1) and life-threatening syndromes like leukocyte adhesion deficiency (2). Activation of adhesion molecules generally involves both modulation of affinity and avidity. The affinity of adhesion molecules often reflects a specific conformation of the extracellular ligand-binding domain. Avidity modulation involves changes in the cell surface distribution of adhesion molecules (*e.g.* lateral oligomerization), which leads to clusters of molecules and thereby specifically increases the number of available receptors at the site of cell-cell interaction.

Activated leukocyte cell adhesion molecule (ALCAM/MEMD/CD166)[1] is a type I transmembrane protein and a member of the Ig superfamily. It has over 90% homology with the chicken adhesion molecule BEN/SC1/DM-GRASP (3–5), and it has 30% identity and 50% similarity with the human melanoma cell adhesion molecule Mel-CAM/MUC18/CD146 (6). Furthermore, ALCAM has 93% sequence identity with the candidate liver high density lipoprotein receptor HB2 (7). ALCAM is involved in various physiological processes including hematopoiesis (8, 9), thymus development (10), the immune response (11), neurite extension (12), neural cell migration (13), and osteogenesis (14).

ALCAM has a short cytoplasmic tail and its extracellular part comprises five Ig domains: two amino-terminal variable (V) type Ig domains followed by three constant (C) type Ig domains ($V_1V_2C_1C_2C_3$). ALCAM was first identified as a CD6 ligand (15), but it also mediates homophilic ALCAM-ALCAM interactions. While the heterophilic ALCAM-CD6 interaction is extensively studied and mapped (16–18), little is known about the molecular basis for the homophilic ALCAM-ALCAM interaction as observed in human melanoma (19, 20) and hematopoiesis (8, 9).

Previously, we have shown that homophilic ALCAM-mediated cell-cell adhesion is regulated through actin cytoskeleton-dependent clustering of ALCAM molecules at the cell surface and that this clustering is necessary to obtain stable adhesive interactions (21). In analogy with other members of the immunoglobulin superfamily like NCAM (22) and Ng-CAM/L1-CAM (23), it is likely that the formation of ALCAM *cis*-homo-oligomers at the cell surface is essential for strong ligand binding and homophilic interactions.

Here we describe a detailed molecular analysis of the homophilic ALCAM interaction and the construction of an amino-terminally deleted ALCAM molecule that inhibited wild-type ALCAM-mediated aggregation in a dose-dependent manner. These combined data lead us to propose a model for homophilic ALCAM-mediated cell adhesion.

MATERIALS AND METHODS

Cell Lines—The adherent human melanoma cell lines BLM and 530 (24) were grown as monolayers in Dulbecco's modified Eagle's medium as described before (19). The erythroleukemia cell line K562 growing in suspension and ALCAM-transfected K562 cells were cultured as described previously (21). Regular tests confirmed that cell lines were free of mycoplasma contamination.

Monoclonal Anti-ALCAM Antibodies—Anti-ALCAM antibody J4-81 (MA250020, IgG1) was purchased from Antigenix America Inc. (Franklin Square, NY). Monoclonal anti-ALCAM antibody AZN-L50 (IgG2a)

* The costs of publication of this article were defrayed in part by the payment of page charges. This article must therefore be hereby marked "*advertisement*" in accordance with 18 U.S.C. Section 1734 solely to indicate this fact.

§ These two authors contributed equally to this work.

** To whom correspondence should be addressed. Tel.: 31-24-3616619; Fax: 31-24-3540525; E-mail: G.Swart@bioch.kun.nl.

[1] The abbreviations used are: ALCAM, activated leukocyte cell adhesion molecule; FITC, fluorescein isothiocyanate; mAb, monoclonal antibody; NCAM, neural cell adhesion molecule.

was generated by immunization of BALB/c mice with K562-ALCAM cells. Four consecutive days before fusion, mice were boosted intravenously. The spleen was isolated, and spleen cells were fused with SP2/0 cells using standard technology. Supernatants of growing hybridomas were tested in a cell enzyme-linked immunosorbent assay using K562-ALCAM cells and K562 cells as a positive and negative control, respectively. Positive hybridomas were recloned several times to obtain true monoclonal hybridomas. The hybridoma AZN-L50 was selected for its strong and specific binding to ALCAM and its ability to inhibit the homophilic ALCAM-ALCAM interaction.

Plate Adhesion Assay—ALCAM-Fc recombinant protein consisting of the five extracellular domains of ALCAM fused to the human IgG1 Fc domain was produced and purified as described earlier (21). Adhesion of cells to immobilized ALCAM-Fc was tested as described before (21). Briefly, flat bottom maxisorp 96 wells plates (NUNC, Roskilde, Denmark) were coated with 4 μg/ml goat anti-human-Fc-F(ab′)$_2$ in TSM (20 mM Tris, 150 mM NaCl, 1 mM $CaCl_2$, 1 mM $MgCl_2$, pH 8.0) for 1 h. Plates were blocked with 1% (w/v) bovine serum albumin in TSM and subsequently coated with 250 ng/ml ALCAM-Fc for 1 h. Cells (2×10^4 cells/well) were labeled with Calcein-AM (Molecular Probes, Inc., Eugene, OR) and preincubated with monoclonal anti-ALCAM antibody J4-81 (5 μg/ml) and/or AZN-L50 (10 μg/ml) for 5–10 min at room temperature. Cells were allowed to adhere in triplicate wells of the coated plates for 20 min (530 cells) or 45 min (KG1, K562-ALCAM) in culture medium at the indicated temperatures. Nonadherent cells were removed by washing the wells five times with TSM plus 0.5% bovine serum albumin at 37 °C. Cells were lysed with lysis buffer (50 mM Tris, 0.1% SDS), and fluorescence was quantified in a cytofluorometer (PerSeptive Biosystems). Adhesion was expressed as the percentage (mean ± S.D.) bound cells of the total cells allowed to adhere in triplicate wells.

Soluble ALCAM-Fc Binding Assay—For soluble ALCAM-Fc binding, the indicated concentrations of ALCAM-Fc were added to 5×10^4 cells in culture medium in V-bottom wells in a final volume of 50 μl. After an incubation of 30 min at 37 °C, cells were washed once with prewarmed (37 °C) medium and subsequently incubated with a fluorescein isothiocyanate (FITC)-conjugated secondary goat anti-human Fc antibody (Cappel Inc., West Chester, PA) in medium for 15 min at 37 °C. After washing with prewarmed medium, cells were analyzed on a FACScan (Becton Dickinson, Mountain View, CA). The mean fluorescence intensity is a measure for the amount of ALCAM-Fc molecules bound to the cells. The percentage of cells that have bound ligand was determined.

Construction of Amino-terminally Truncated ALCAM Mutants—Amino-terminally truncated ALCAM mutants were generated using the polymerase chain reaction and carefully chosen restriction sites in pWD201 (2.1-kilobase pair ALCAM cDNA coding for the leader sequence, the two V-type and three C-type Ig domains, the transmembrane spanning domain, and the short cytoplasmic tail ($V_1V_2C_1C_2C_3$) in pZip-neo-(X)-1 containing the neomycin resistance gene (19)). A schematic representation is shown in Fig. 1. The ALCAM leader sequence was amplified using a 5′ Rev/T3 primer (5′-ATT ACG CCA AGC TCG AA-3′) and 3′ primers extended with a suitable restriction site. For the generation of pWD277 ($V_2C_1C_2C_3$-construct), the Rev/T3 and P9-*Pst*I (5′-AG CAT GCC AGA AGG TAT GAT AAT GGT ATC TCC ATA T-3′) primer pair was used to amplify the leader sequence. The amplified fragment was subsequently cloned in *Sst*I/*Pst*I-linearized pWD201. For the generation of pWD275 ($C_1C_2C_3$ construct), the leader was amplified using the Rev/T3 and P8-*Bal*I (5′-CTG GCC AGA AGG TAT GAT AAT GGT ATC TCC ATA T-3′) primer pair and cloned in *Sst*I/*Bal*I-linearized pWD201. Finally, pWD278 (C_2C_3 construct) was generated using the Rev/T3 and P7-*Nhe*I (5′-GCT AGC AGA TAT TGT GCA AGG TAT GAT AAT GGT ATC TCC ATA T-3′) primer pair. Thereafter, the fragment was cloned in *Sst*I/*Nhe*I-linearized pWD201. The sequences of all constructs were verified.

Transfection—FuGENE-6 transfection reagent (Roche Molecular Biochemicals) was used to transfect the human melanoma cell lines according to the manufacturer's protocol. In brief, a mixture of FuGENE-6 and circular DNA (3 μl and 0.5 μg, respectively) was added dropwise to a 40% confluent monolayer in a six-well plate in medium. After 48 h, medium was replaced with selection medium (medium plus 1 mg/ml G418 (Life Technologies, Inc.)). Neomycin-resistant colonies were expanded and maintained in medium supplemented with 0.5 mg/ml G418.

Flow Cytometry: Cell Surface Expression and Aggregation Assay—Cells (2×10^5) were incubated with the indicated mouse monoclonal antibody at 4 μg/ml in PBA (phosphate-buffered saline containing 1% bovine serum albumin and 0.05% NaN_3) for 30 min at 4 °C, washed three times with PBA, and further incubated with FITC-conjugated goat anti-mouse IgG antibody (Dako, Glostrup, Denmark) for 30 min at 4 °C. After washing, positive cells were detected using a FACScan, and the mean fluorescence intensity was determined.

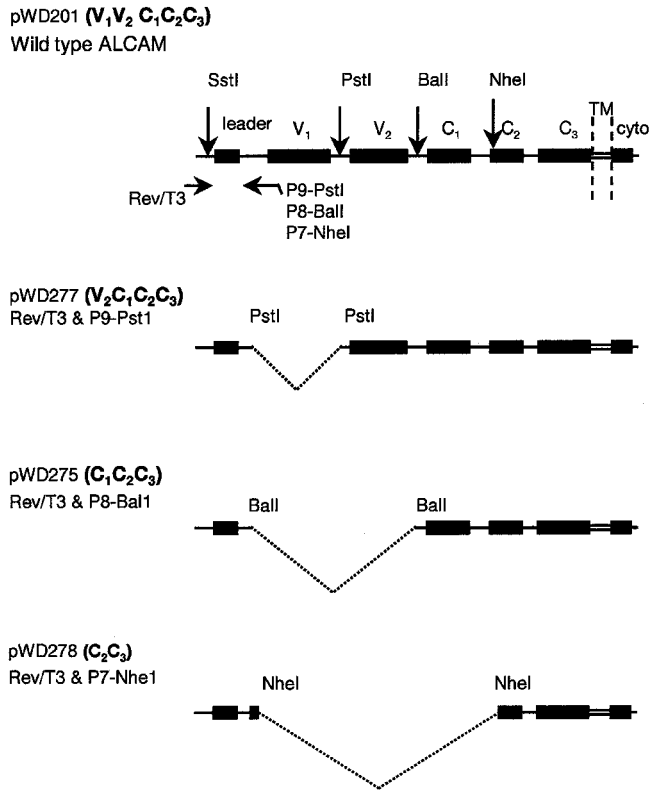

FIG. 1. **Construction of NH_2-terminally truncated ALCAM mutants.** Using the polymerase chain reaction and standard cloning procedures, deletion mutants of ALCAM were made as described under "Materials and Methods." Primers P9, P8, and P7 contained a *Pst*I, *Bal*I, and *Nhe*I restriction site respectively, which facilitated cloning of the generated fragment into double-digested ALCAM cDNA (pWD201) at the *Sst*I and the respective restriction enzyme site. *V_1* and *V_2*, V-type domains; *C_1*, *C_2*, and *C_3*, C-type domains; *TM*, transmembrane domain; *cyto*, cytoplasmic tail; *P7*, *P8*, and *P9*, primers 7–9; *Rev/T3*, reverse T3 primer.

The aggregation capacity of human melanoma cell lines was measured by a double colored assay as described previously (19). Briefly, two separate cell suspensions were labeled fluorescent green or fluorescent red with 5,6-sulfofluorescein diacetate (50 μg/ml in culture medium; Molecular Probes) or hydroethidine (40 μg/ml in culture medium; Plysciences, Warrington, PA), respectively. Following extensive washing, cells were mixed in equal amounts and allowed to aggregate at 37 °C for 30 min. After incubation, cells were fixed by adding paraformaldehyde to a final concentration of 0.5% (w/v) and subsequently analyzed using a FACScan. Aggregation was expressed as the percentage of double colored events of the total events.

Immunofluorescence—Immunofluorescence was performed on methanol/acetone-fixed monolayers of cells grown on a glass surface as described previously (19). Affinity-purified mouse monoclonal antibodies were used at 4 μg/ml in phosphate-buffered saline.

Western Blotting—Cells (7×10^6) were lysed for 30 min on ice in 1 ml of lysis buffer (25 mM Tris-HCl, pH 7.5, 1% Nonidet P-40, 100 mM KCl, 10 mM $MgCl_2$, 0.25 mM dithioerythritol, 1 mM phenylmethylsulfonyl fluoride, 1 mM benzamidine, 2 mM Na_2VO_4, 10 μg/ml leupeptin, 10 μg/ml aprotinin). Nuclei and the Nonidet P-40 insoluble fraction were spun down at maximum speed in an Eppendorf centrifuge. Supernatants were stored at −80 °C.

Protein concentration was determined using the Bio-Rad protein assay and reagents according to the supplier's instructions. Equal amounts of protein were subjected to 6.5% SDS-polyacrylamide gel electrophoresis and subsequently transferred to Hybond-C pure membrane (Amersham Pharmacia Biotech). Membranes were blocked for 1 h at room temperature in Tris-buffered saline containing 0.05% Tween 20 (TBS-T) and 5% (w/v) low fat milk powder. After washing the membranes three times with TBS-T, the blots were incubated with AZN-L50 (3 μg/ml in TBS-T supplemented with 3% (w/v) low fat milk powder) for

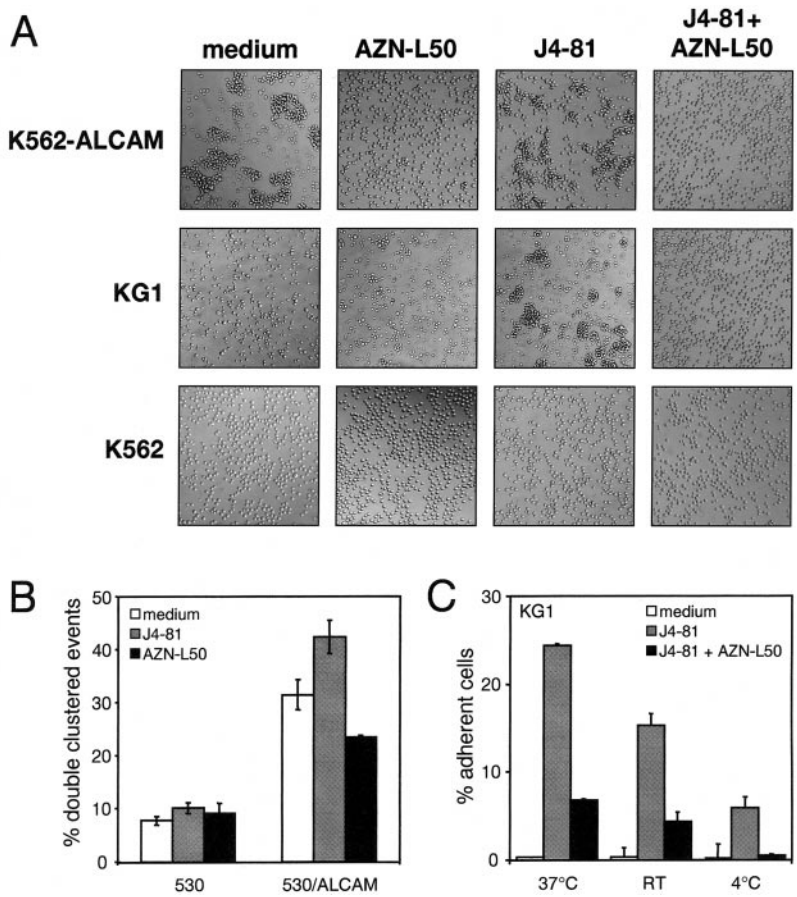

FIG. 2. **Monoclonal anti-ALCAM antibodies have differential effects on ALCAM-mediated cell aggregation and adhesion.** *A*, phase-contrast microscopy. Ectopic ALCAM expression in erythroleukemic K562 cells (K562-ALCAM) induced cell aggregation in culture, whereas vector control K562 cells did not aggregate. mAb J4-81(5 μg/ml) could not further enhance this spontaneous aggregation, but the ALCAM-mediated aggregation was efficiently inhibited by the mAb AZN-L50 (10 μg/ml). Both antibodies had no effect on vector control K562 cells. Aggregation of wild-type ALCAM-expressing myelomonocytic KG1 cells significantly increased upon treatment with mAb J4-81. This J4-81-induced cell aggregation was completely inhibited with mAb AZN-L50. *B*, cell-cell aggregation in the absence or presence of an anti-ALCAM mAb was quantified by two-color flow cytometry. mAb J4-81 (5 μg/ml) increased the cell aggregation of the ectopically ALCAM-expressing human melanoma cell line 530/ALCAM with 35% as compared with the untreated cells, while mAb AZN-L50 (5 μg/ml) reduced this aggregation with 25% with respect to the untreated control. Neither of the antibodies had any effect on the ALCAM-negative vector control cell line. Increasing concentrations of mAb AZN-L50 up to 10 μg/ml did not further reduce the cellular aggregation (not shown). *C*, myelomonocytic KG1 cells were allowed to adhere to immobilized recombinant human ALCAM-Fc, in the presence or absence of the ALCAM mAb J4-81 (5 μg/ml) or AZN-L50 (10 μg/ml) at the indicated temperatures, and the percentage of adhering cells was determined. ALCAM-mediated cell adhesion was strongly induced by mAb J4-81. This J4-81-induced adhesion was efficiently inhibited when tumor cells were incubated with mAb AZN-L50 (10 μg/ml) prior to adhesion. mAb-induced adhesion required physiological temperature, since it was clearly inhibited at lower temperatures, indicating that J4-81 induction of adhesion is not due to cross-linking of opposing ALCAM molecules.

2 h at room temperature. Following three washes with TBS-T at room temperature, the membranes were incubated with horseradish peroxidase-conjugated rabbit anti-mouse IgG (1:2000, Dako, Glostrup, Denmark) in TBS-T plus 5% milk powder for 1 h at room temperature. After three washes with TBS-T, proteins were visualized via the enhanced chemiluminescent reaction (Amersham Pharmacia Biotech).

RESULTS

Monoclonal Anti-ALCAM Antibodies Have Differential Effects on ALCAM-mediated Cell Aggregation and Adhesion—To elucidate the molecular mechanism underlying the homophilic ALCAM-ALCAM interaction, the availability of function blocking monoclonal antibodies (mAbs) is virtually indispensable. The ALCAM-antibody J4-81 has previously been described to block heterophilic ALCAM-CD6 interactions (25). In contrast to these findings, we observed that the addition of mAb J4-81 markedly increased homotypic cell clustering of ALCAM-positive but CD6-negative myelomonocytic KG1 cells (Fig. 2*A*). Therefore, new mAbs were generated and selected for the capacity to specifically inhibit homophilic ALCAM-ALCAM interactions. ALCAM mAb AZN-L50 completely inhibited the J4-81-induced homotypic cell clustering of KG1 cells to background levels (Fig. 2*A*). Ectopic expression of ALCAM in erythroleukemic K562 cells (K562-ALCAM) resulted in the occurrence of large ALCAM-mediated cell clusters in suspension that were not observed in the parental K562 cells. While the addition of mAb J4-81 could not further enhance cell clustering of K562-ALCAM cells, mAb AZN-L50 completely blocked the spontaneous ALCAM-dependent cell clustering of these cells (Fig. 2*A*). Neither mAb J4-81 nor AZN-L50 had any effect on ALCAM-negative parental K562 cells (Fig. 2*A*).

Using human melanoma 530 cells, similar activating and inhibiting effects of the monoclonal antibodies on ALCAM-mediated aggregation were observed in an aggregation assay analyzed by flow cytometry. While parental 530 cells do not express ALCAM and do not aggregate, aggregation of these cells is induced by ectopic expression of ALCAM (530/$V_1V_2C_1C_2C_3$) (19), and this clustering was further increased by 35% using mAb J4-81, whereas mAb AZN-L50 inhibited the ALCAM-mediated aggregation by 25% as compared with the untreated control (530/ALCAM) (Fig. 2*B*). Neither of the antibodies had any effect on the ALCAM-negative vector control 530 cells that did not aggregate (Fig. 2*B*). A similar pattern of

activation and blocking of adhesion by these mAbs was observed when using the human melanoma cell line BLM expressing endogenous ALCAM (not shown).

In addition to cell-cell aggregation assays, we analyzed the effect of mAbs J4-81 and AZN-L50 on ALCAM-mediated stable cell adhesion to immobilized recombinant ALCAM-Fc. KG1 cells were allowed to adhere to an ALCAM-Fc-coated surface in the presence or absence of ALCAM mAbs J4-81 and AZN-L50. No ALCAM-mediated adhesion was observed in the absence of mAbs. The addition of mAb J4-81 induced adhesion of KG1 to immobilized ALCAM-Fc, which in turn was efficiently inhibited by the addition of the function blocking mAb AZN-L50 at physiological temperatures (Fig. 2*C*). To exclude the possibility that mAb J4-81 enhanced cellular aggregation and adhesion via cross-linking of two ALCAM molecules on opposing cells (or immobilized ALCAM-Fc), adhesion of KG1 to immobilized ALCAM-Fc was performed at lower, nonphysiological temperatures (Fig. 2*C*). The strong induction of ALCAM-mediated adhesion of KG1 cells by mAb J4-81 was temperature-dependent as the observed adhesion was reduced when cell adherence was performed at room temperature or at 4 °C. Furthermore, the adhesion of KG1 cells induced by mAb J4-81 is efficiently blocked with mAb AZN-L50 (Fig. 2*C*). Similar results were obtained with K562-ALCAM cells (not shown). Thus, a pair of monoclonal antibodies was characterized that either activated (J4-81) or blocked (AZN-L50) the homophilic ALCAM-ALCAM interaction.

Domain Mapping of mAbs J4-81 and AZN-L50 to Specific Ig Domains of ALCAM—The results of these functional studies with mAbs are more informative when the respective antibody epitopes are known. To identify the Ig domains that are involved in the homophilic ALCAM-mediated interactions, domain mapping was performed for mAbs J4-81 and AZN-L50. A series of progressively amino-terminally truncated ALCAM mutants was generated and expressed in the ALCAM-negative human melanoma cell line 530. The extracellular part of wild-type ALCAM consists of two amino-terminal V-type domains and three membrane-proximal C-type domains (*i.e.* $V_1V_2C_1C_2C_3$). Immunofluorescence analysis was performed with the anti-ALCAM antibodies on the transfected cells to identify the domains required for antibody recognition (Table I). mAb J4-81 only recognized wild-type ALCAM, while mAb AZN-L50 recognized all available ALCAM constructs. Thus, the epitope for anti-ALCAM mAb J4-81 is mapped to domain V_1, whereas that for AZN-L50 is located in the C_2C_3 module of ALCAM.

The Amino-terminal Ig Domain V_1 of ALCAM Is Required for Ligand Binding and Homophilic Cell-Cell Interactions—The adhesion, aggregation, and antibody mapping data obtained from experiments using mAbs AZN-L50 and J4-81 (Fig. 2 and Table I) suggest that the membrane-proximal domains C_2C_3 and the amino-terminal domain V_1 are directly involved in homophilic ALCAM-ALCAM interactions. To further explore the role of domain V_1 in ALCAM-mediated aggregation, the series of amino-terminally truncated ALCAM mutants expressed in the ALCAM-negative human melanoma cell line 530 were subjected to flow cytometry to determine the cell surface expression of the truncated ALCAM molecules, using mAb AZN-L50 that recognizes the membrane-proximal domains C_2C_3 of ALCAM (Fig. 3*A*). The ALCAM mutant lacking domains $V_1V_2C_1$ did not localize at the cell surface; therefore, this mutant was not included in the subsequent aggregation assay. Deletion of domain V_1 reduced the aggregation capacity to the background levels observed in the control 530 cells transfected with empty vector (Fig. 3*B*). In addition, the cell lines expressing truncated ALCAM did not aggregate with cells expressing wild-type ALCAM (not shown). From these findings, we conclude that domain V_1 is essential in mediating homophilic ALCAM interactions.

TABLE I
Immunofluorescence-based epitope mapping of two monoclonal anti-ALCAM antibodies

NH_2-terminally truncated ALCAM mutants were ectopically expressed in the ALCAM-negative cell line 530. Immunofluorescence was performed employing the mAb AZN-L50 (4 μg/ml) and J4–81 (4 μg/ml) on methanol/acetone-fixed cells grown on glass coverslips. The epitopes for AZN-L50 and J4–81 reside in the C_2C_3 Ig domains and V_1 Ig domain, respectively. Full-length ALCAM ($V_1V_2C_1C_2C_3$) and the truncated mutants $V_2C_1C_2C_3$ and $C_1C_2C_3$ were membranously expressed, whereas expression of the truncated mutant C_2C_3 was restricted to the cytoplasm.

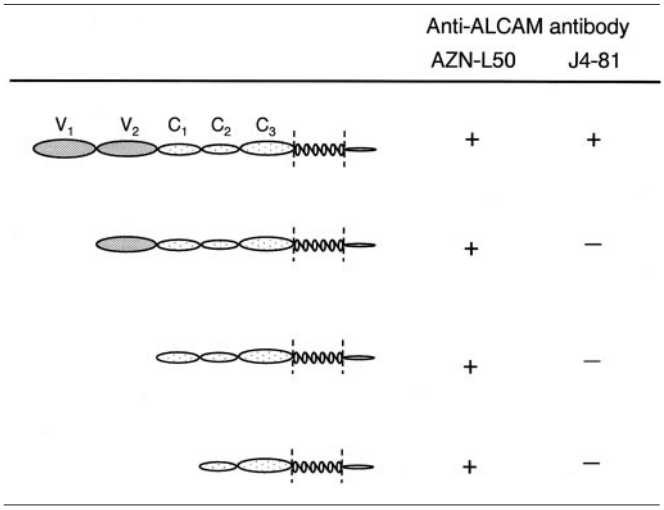

Binding of soluble ALCAM-Fc by ALCAM-expressing cells is a sensitive assay to assess the ALCAM ligand binding capacity, *i.e.* the affinity. The ligand binding capacity of the amino-terminally truncated ALCAM molecules was compared with that of wild-type ALCAM. In line with the results of the cell aggregation assays, this assay also revealed that deletion of the amino-terminal domain V_1 from the cell surface-expressed ALCAM (530/$V_2C_1C_2C_3$) completely abolished binding of soluble ALCAM-Fc as compared with 530 melanoma cells ectopically expressing wild-type ALCAM (530/$V_1V_2C_1C_2C_3$) (Fig. 3*C*). Moreover, 530 cells expressing amino-terminally truncated ALCAM did not adhere to immobilized ALCAM-Fc at all, while 530 cells expressing wild-type ALCAM were readily activated to adhere to ALCAM-Fc by the addition of mAb J4-81 (Fig. 3*D*). Furthermore, the function-blocking mAb AZN-L50 (10 μg/ml), which maps to the membrane-proximal domains C_2C_3, did not affect soluble ligand binding affinity by K-ALCAM cells (Fig. 4), whereas it completely inhibited aggregation of these cells in suspension (Fig. 2*A*) at the same concentration. Although the half-maximum ligand-binding value moderately increased from 1.5 to 3.5 μg/ml in the presence of AZN-L50, this slight decrease in ligand binding cannot account for the complete AZN-L50-induced inhibition of cellular aggregation of K-ALCAM cells in suspension. In conclusion, the membrane-distal domain V_1 is critically involved in ligand binding and in mediating stable ALCAM mediated cell-cell adhesion.

Involvement of the Membrane-proximal Domains C_2C_3 of ALCAM in Homophilic Cell-Cell Interactions—In addition to the involvement of domain V_1 in ALCAM-mediated aggregation and adhesion, the specific inhibition of homophilic ALCAM interactions by mAb AZN-L50 suggests that the membrane-proximal domains C_2C_3 might be equally important in the formation of stable cell-cell interactions. Previously, it was

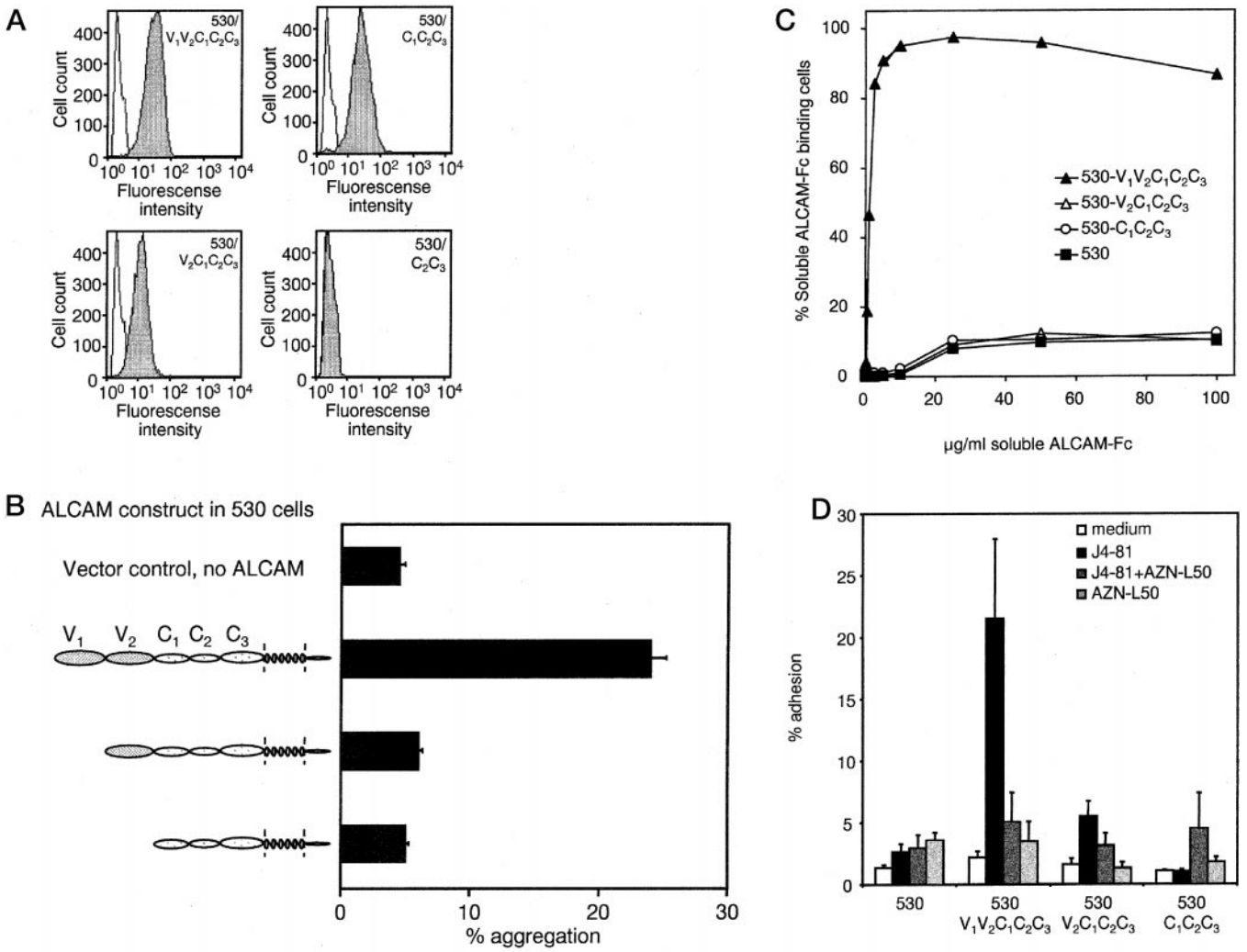

FIG. 3. **The amino-terminal V-type Ig domain (V_1) is essential for ligand binding and ALCAM-mediated cell aggregation.** *A*, cell surface expression levels of wild-type ALCAM and truncated ALCAM mutants in the ALCAM-negative human melanoma cell line 530 were determined by flow cytometry employing the mAb AZN-L50 (4 µg/ml), which recognizes all mutants, since its epitope resides in the membrane-proximal domains C_2C_3. *Open histograms* represent the isotype control staining, and the *gray histograms* represent the AZN-L50 staining of wild type and truncated ALCAM. The constructs lacking the first or both V-type Ig domains, $V_1C_1C_2C_3$ or $C_1C_2C_3$ respectively, were expressed at the cell surface. The construct C_2C_3 lacking both V-type Ig domains and the first C-type Ig domain did not localize to the cell surface. *B*, cell lines expressing wild-type or mutant ALCAM were subjected to an aggregation assay and quantified by flow cytometry. Wild-type or NH_2-terminally truncated ALCAM molecules were expressed in the ALCAM-negative melanoma cell line 530. Cells expressing wild type ALCAM aggregated strongly, while truncation of the first amino-terminal domain V_1 already completely abrogated cell aggregation. Subsequent deletion of more domains did not have an additional effect on inhibition of adhesion. *C*, cells (530/$V_1V_2C_1C_2C_3$, 530/truncated ALCAM) were incubated with soluble ALCAM-Fc at 37 °C, and bound ALCAM-Fc was detected with a FITC-conjugated anti-human-Fc antibody. The percentage of cells that had bound ligand was determined by flow cytometry. The ectopically ALCAM-expressing cell line 530/$V_1V_2C_1C_2C_3$ could efficiently bind soluble ALCAM-Fc in a concentration-dependent manner. In contrast, ALCAM-negative 530 vector control cells (530) and 530 cells expressing truncated ALCAM (530/$V_2C_1C_2C_3$ and 530/$C_1C_2C_3$) did not bind soluble ALCAM-Fc. *D*, 530 cells, or 530 cells expressing wild-type or truncated ALCAM mutants were allowed to adhere to immobilized recombinant human ALCAM-Fc, in the presence or absence of the ALCAM mAb J4-81 (5 µg/ml) or AZN-L50 (10 µg/ml), and the percentage of adhering cells was determined. Wild-type ALCAM-expressing 530 cells were readily activated to adhere to ALCAM-Fc by the addition of mAb J4-81, and J4-81-induced adhesion was inhibited by the addition of AZN-L50. ALCAM mutants lacking the membrane-distal domain V_1 or control-transfected 530 control cells did not adhere to immobilized ALCAM-Fc, and adhesion could not be induced by the addition of J4-81.

shown that increased clustering of ALCAM molecules at the cell membrane enhanced avidity, which was required for stable ALCAM-mediated adhesion (21). To explore the effects of partly deleting the ligand binding domain in these ALCAM complexes on ALCAM-mediated cell aggregation, amino-terminally truncated ALCAM ($C_1C_2C_3$ = ΔN-ALCAM) was introduced into BLM melanoma cells expressing wild-type ALCAM by stable transfection. Three independently isolated transfected cell clones (BLM/ΔN-ALCAM-1, BLM/ΔN-ALCAM-2, and BLM/ΔN-ALCAM-3) with different ΔN-ALCAM expression levels were selected for further analysis. Overexpression of ΔN-ALCAM led to a decreased aggregation capacity of the BLM cells in a dose-dependent manner (Fig. 5, *A* and *B*), despite unaltered expression levels of wild-type ALCAM molecules (Fig. 5*A*). Therefore, elimination of domains V_1V_2 of ALCAM generates a dominant negative ALCAM molecule with respect to ALCAM-mediated homophilic cell aggregation when introduced in cells expressing wild-type ALCAM. To analyze whether the introduction of ΔN-ALCAM influenced the ligand binding affinity of wild-type ALCAM, the soluble ligand binding capacity of wild-type ALCAM-expressing BLM cells co-expressing ΔN-ALCAM was compared with parental BLM cells. The BLM cell lines expressing ΔN-ALCAM did not show a reduction in their capacity to bind soluble ALCAM-Fc com-

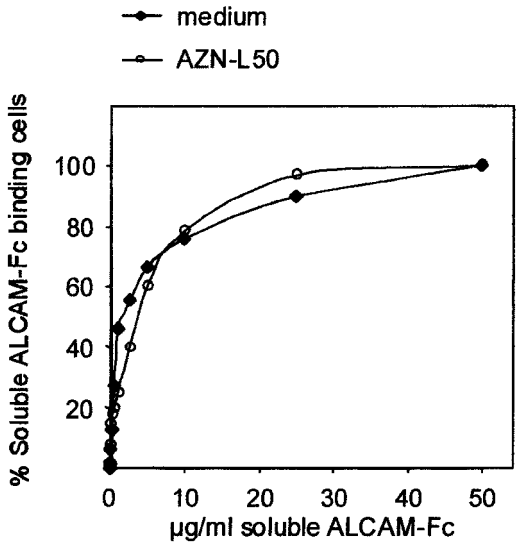

FIG. 4. **Aggregation blocking mAb AZN-L50 slightly reduced the soluble ALCAM-Fc ligand-binding capacity of K562-ALCAM cells.** Cells (K562-ALCAM) were incubated with soluble ALCAM-Fc in the presence or absence of the aggregation-blocking mAb AZN-L50 (10 μg/ml). The percentage of cells that have bound ALCAM-Fc was determined by flow cytometry using a FITC-conjugated anti-human-Fc antibody. mAb AZN-L50 moderately increased the half-maximum ligand-binding capacity from 1.5 to 3.5 μg/ml, indicative of a marginally reduced ligand binding capacity.

pared with the control BLM cells transfected with the empty expression vector (BLM) (Fig. 5*C*). Control cells (BLM) and cells transfected with truncated ALCAM (BLM/ΔN-ALCAM) displayed similar apparent half-maximal ligand-binding values (1.6 and 1.3 μg/ml, respectively). This strongly indicates that the decreased aggregation capacity of the ΔN-ALCAM-expressing cells is due to a decrease in wild-type ALCAM avidity rather than a decrease in the ligand binding capacity.

DISCUSSION

Heterophilic interactions between ALCAM and CD6 have been extensively studied and mapped (18, 26). In contrast, the molecular basis for homophilic ALCAM-ALCAM interactions has remained largely elusive. Functional homophilic ALCAM-mediated adhesion was demonstrated for melanoma cells (19) and hematopoietic cells (8). Recently, we have shown that ALCAM-mediated homophilic adhesion is dynamically regulated through the actin cytoskeleton (21). However, the involvement of specific domains in ALCAM-ALCAM-mediated adhesion had not been addressed yet.

Here we have shown that wild-type ALCAM ($V_1V_2C_1C_2C_3$) is bimodular, consisting of a distinct ligand binding module comprising the membrane-distal domain V_1 and an oligomerization module comprising the membrane-proximal C-type domains C_2C_3. Both modules are required for stable cell adhesion and aggregation. We propose a molecular model that accounts for the observed properties of homophilic ALCAM interactions (Fig. 6).

Using a series of progressively amino-terminally truncated ALCAM mutants, we found that the amino-terminal domain V_1 is critically involved in the homophilic interaction. Deletion of domain V_1 not only disrupted the homophilic ALCAM-mediated cell-cell interaction but also completely prevented binding of soluble wild-type ALCAM-Fc. These observations indicated that a direct and exclusive interaction between two opposing domains V_1 is crucial for homophilic ALCAM-mediated adhesion. If multiple Ig domains were directly involved in the homophilic ALCAM interaction, cells expressing an ALCAM construct that solely lacks domain V_1 would be expected to display

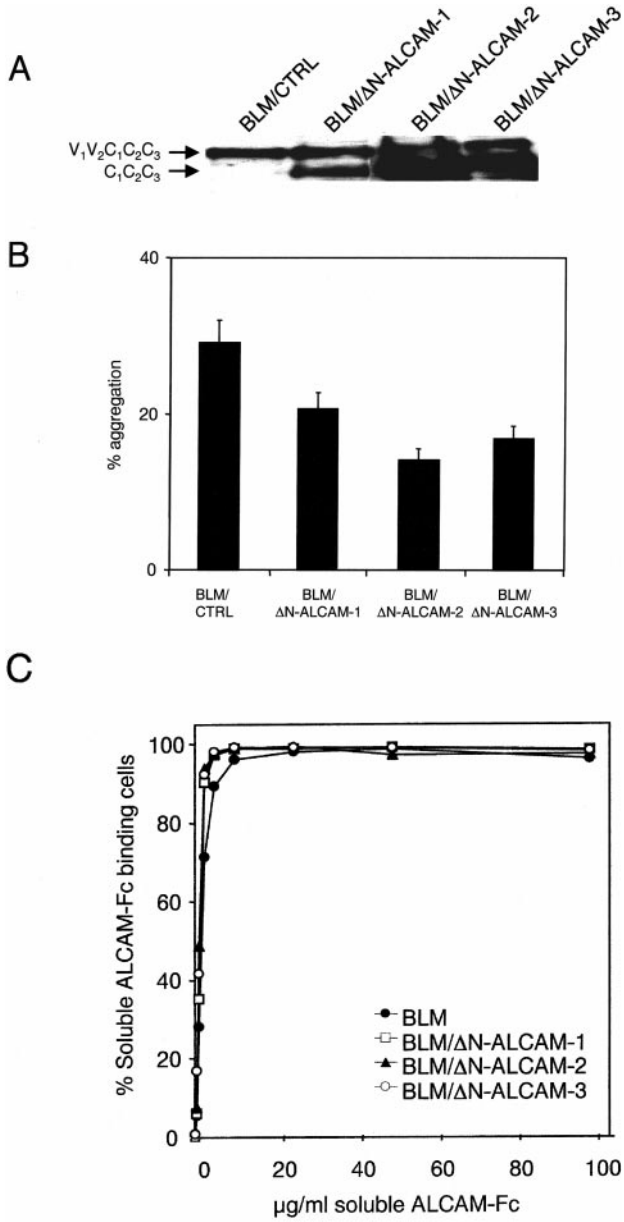

FIG. 5. **ΔN-ALCAM ($C_1C_2C_3$), expressed in the wild-type ALCAM-expressing cell line BLM, reduced cell aggregation in a dose-dependent fashion without affecting soluble ligand binding affinity.** Cell clones overexpressing amino-terminally truncated ALCAM (ΔN-ALCAM) were generated from the parental cell line BLM with endogenous ALCAM expression by stable transfection. Three independently isolated cell clones (BLM/ΔN-ALCAM-1, -2, and-3) expressing different levels of ΔN-ALCAM were selected for further analysis. *A*, expression levels of the truncated molecule were determined by Western blotting using mAb AZN-L50 (3 μg/ml) that recognizes the membrane-proximal Ig domains C_2C_3. The three established cell lines showed different expression levels of the truncated ALCAM molecule, while expression of the wild-type ALCAM molecule remained unaltered. *B*, the established cell lines expressing truncated ALCAM (BLM/ΔN-ALCAM -1, -2, and -3) were subjected to an *in vitro* aggregation assay and analyzed by two-color flow cytometry. Expression of truncated ALCAM reduced the aggregation capacity of these cells as compared with the vector control cell line (BLM/CTRL) in a dose-dependent manner, and thus truncated ALCAM ($C_1C_2C_3$) functions as a dominant negative molecule with respect to wild-type ALCAM mediated aggregation. *C*, cells (BLM, BLM/ΔN-ALCAM-1, -2, and -3) were incubated with soluble ALCAM-Fc. The percentage of cells that have bound ALCAM-Fc was determined by flow cytometry using a FITC-conjugated anti-human Fc antibody. Ectopic ΔN-ALCAM expression in BLM cells with wild-type ALCAM did not affect the capacity to bind soluble ALCAM-Fc ligand, demonstrating that ectopic expression of ΔN-ALCAM does not change the affinity of endogenously expressed ALCAM for soluble ALCAM-Fc.

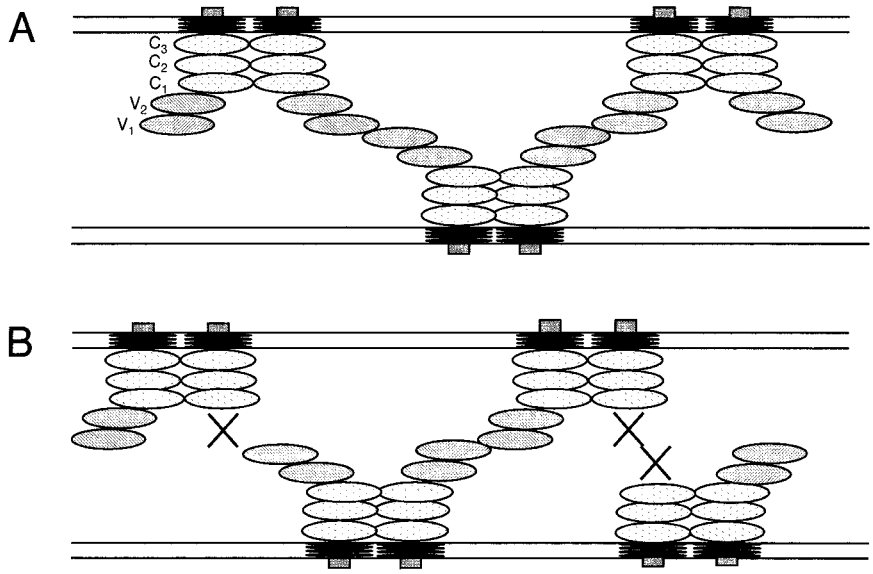

FIG. 6. **Model for the oligomeric homophilic ALCAM-ALCAM interaction.** *A*, the membrane-proximal C-type Ig domains are involved in lateral oligomerization of ALCAM, which is inhibited with the anti-C_2C_3 mAb AZN-L50, while the NH_2-terminal domain V_1 mediates the actual homophilic interaction. Deletion of domain V_1 resulted in a molecule that cannot bind soluble ALCAM and, therefore, has lost the ability to mediate cell aggregation. For reasons of simplicity, the formation of a dimer is shown, but the actual mechanism could involve the formation of higher oligomers of multiple ALCAM molecules, creating a two-dimensional lattice. *B*, a model for the dominant negative effect of truncated ALCAM. Overexpression of $C_1C_2C_3$ ALCAM in cells already expressing wild type ALCAM results in the formation of hetero-oligomers of wild-type and truncated ALCAM molecules and subsequently interferes in the tight ALCAM network formation because only isolated ligand binding domains V_1 are exposed instead of oligomers. Expression of the truncated molecule will reduce but not completely inhibit the ALCAM-mediated aggregation via the Ig domain V_1, because ligand-binding modules are still provided by the endogenously expressed wild-type ALCAM.

a residual capacity to aggregate with cells expressing wild-type ALCAM. Moreover, truncated ALCAM-expressing cells would be expected to bind soluble wild-type ALCAM, albeit at lower affinity, if additional domains were involved in ligand binding. However, both cell-cell aggregation and soluble ligand binding were completely abolished upon deletion of the amino-terminal domain V_1. Furthermore, mAb AZN-L50, which maps to the membrane-proximal domains C_2C_3, only slightly decreased the soluble ligand binding affinity, whereas it completely inhibited aggregation of these cells in suspension at the same concentration (10 μg/ml). It is therefore unlikely that the slight decrease in soluble ligand binding (*i.e.* increase in half-maximal ligand-binding value from 1.5 to 3.5 μg/ml in the presence of AZN-L50) accounted for the total inhibition of ALCAM-mediated cellular aggregation via AZN-L50. Thus, these data indicate that ligand binding in itself is independent of the C-type Ig domains and that homophilic ALCAM-ALCAM *trans*-interactions are exclusively mediated by binding of opposing amino-terminal V_1 domains.

mAb J4-81, which specifically recognizes domain V_1, enhanced homophilic ALCAM-mediated cell adhesion and aggregation, possibly by inducing a conformational change that promotes ligand binding. KG1 cells with abundant ALCAM cell surface expression were only able to form homotypic cell clusters after activation by mAb J4-81. In contrast, spontaneous cell clustering of K562 cells with ectopic ALCAM expression could not be further enhanced by J4-81 treatment. These findings suggest differential activation of ALCAM in these two cell lines. We could exclude the possibility that mAb J4-81-enhanced aggregation and adhesion to immobilized ALCAM-Fc is caused by cross-linking ALCAM molecules of opposing cells, because the stimulatory effect of mAb J4-81 was temperature-dependent and efficiently inhibited by the blocking anti-ALCAM mAb AZN-L50. The observed enhancement of homophilic ALCAM-mediated adhesion and aggregation by mAb J4-81 is in contrast with the inhibitory effect of this antibody on the heterophilic ALCAM-CD6 interaction (25). This indicates that different mechanisms are regulating the homophilic and heterophilic ALCAM ligand binding interactions.

The inhibitory effect of AZN-L50, which is mapped to the membrane-proximal domains C_2C_3, indicated that these domains are also essential for the homophilic ALCAM-mediated interaction. In analogy with other Ig superfamily molecules like IgG, major histocompatibility complex class II, NCAM (27), and Ng-CAM/L1-CAM (23), these C-type Ig domains are probably involved in the formation of *cis*-homo-oligomers at the cell surface via lateral oligomerization. Aruffo and co-workers (28) have speculated that ALCAM oligomerization might be essential for the heterophilic ALCAM-CD6 interaction. Recently, we have shown that homophilic ALCAM-mediated cell adhesion is regulated through actin cytoskeleton-dependent clustering of ALCAM molecules at the cell surface. The resulting increased avidity of ALCAM clusters is essential to obtain stable adhesive interactions (21). Here we show that expression of ΔN-ALCAM, which lacks the ligand binding domain, in the wild-type ALCAM-expressing BLM cells reduced cell aggregation but not soluble ligand binding. This indicates that ΔN-ALCAM expression changes wild-type ALCAM avidity rather than affinity, suggesting a direct interaction of ΔN-ALCAM with wild-type ALCAM without disturbing soluble ligand binding. In the model proposed in Fig. 6*A*, ALCAM monomers form lateral oligomers via their membrane-proximal C-type domains, whereas the amino-terminal domain V_1 mediates the actual ligand binding. Triggering of lateral oligomerization might be a ligand-induced event, which possibly occurs through a conformational change of ALCAM. This concept is supported by previous findings that in response to ligand binding, the linkage of ALCAM to the actin cytoskeleton is strengthened (21), which can stabilize oligomers at the cell surface. Similar to ligand-induced clustering, mAb J4-81 might induce a conformational change that triggers oligomerization.

Since the epitope for ALCAM-blocking mAb AZN-L50 is localized in domains C_2C_3, it is tempting to speculate that the inhibitory effect of this mAb is a result of prohibited lateral

oligomerization of ALCAM molecules by steric hindrance. This notion is supported by the observation that mAb AZN-L50 does not affect soluble ligand binding (Fig. 4) and therefore only modulates ALCAM avidity. Although inhibition of cell aggregation via ΔN-ALCAM was dependent on its expression level, aggregation could not completely be reduced to background levels. This residual cell-cell aggregation capacity is consistent with the proposed model because some homophilic ALCAM-mediated cell-cell interactions are maintained (Fig. 6*B*).

In conclusion, we have demonstrated that ALCAM-mediated homophilic interactions most likely require lateral homo-oligomerization through the membrane-proximal C-type Ig domains, while the membrane-distal Ig domain V_1 is exclusively involved in ligand binding. Coordinate oligomerization and ligand binding leads to the formation of a tight, bilayered ALCAM network, enabling stable adhesive interactions.

REFERENCES

1. Li, G., and Herlyn, M. (2000) *Mol. Med. Today* **6**, 163–169
2. Etzioni, A. (1994) *Cell Adhes. Commun.* **2,** 257–260
3. Pourquie, O., Corbel, C., Le Caer, J. P., Rossier, J., and Le Douarin, N. M. (1992) *Proc. Natl. Acad. Sci. U. S. A.* **89,** 5261–5265
4. Burns, F. R., von Kannen, S., Guy, L., Raper, J. A., Kamholz, J., and Chang, S. (1991) *Neuron* **7,** 209–220
5. Tanaka, H., Matsui, T., Agata, A., Tomura, M., Kubota, I., McFarland, K. C., Kohr, B., Lee, A., Phillips, H. S., and Shelton, D. L. (1991) *Neuron* **7,** 535–545
6. Lehmann, J. M., Riethmuller, G., and Johnson, J. P. (1989) *Proc. Natl. Acad. Sci. U. S. A.* **86,** 9891–9895
7. Matsumoto, A., Mitchell, A., Kurata, H., Pyle, L., Kondo, K., Itakura, H., and Fidge, N. (1997) *J. Biol. Chem.* **272,** 16778–16782
8. Uchida, N., Yang, Z., Combs, J., Pourquie, O., Nguyen, M., Ramanathan, R., Fu, J., Welply, A., Chen, S., Weddell, G., Sharma, A. K., Leiby, K. R., Karagogeos, D., Hill, B., Humeau, L., Stallcup, W. B., Hoffman, R., Tsukamoto, A. S., Gearing, D. P., and Peault, B. (1997) *Blood* **89,** 2706–2716
9. Cortes, F., Deschaseaux, F., Uchida, N., Labastie, M. C., Friera, A. M., He, D., Charbord, P., and Peault, B. (1999) *Blood* **93,** 826–837
10. Patel, D. D., Wee, S. F., Whichard, L. P., Bowen, M. A., Pesando, J. M., Aruffo, A., and Haynes, B. F. (1995) *J. Exp. Med.* **181,** 1563–1568
11. Levesque, M. C., Heinly, C. S., Whichard, L. P., and Patel, D. D. (1998) *Arthritis Rheum.* **41,** 2221–2229
12. Sekine-Aizawa, Y., Omori, A., and Fujita, S. C. (1998) *Eur. J. Neurosci.* **10,** 2810–2824
13. Heffron, D. S., and Golden, J. A. (2000) *J. Neurosci*. **20**, 2287–2294
14. Bruder, S. P., Ricalton, N. S., Boynton, R. E., Connolly, T. J., Jaiswal, N., Zaia, J., and Barry, F. P. (1998) *J. Bone Miner. Res.* **13,** 655–663
15. Bowen, M. A., Patel, D. D., Li, X., Modrell, B., Malacko, A. R., Wang, W. C., Marquardt, H., Neubauer, M., Pesando, J. M., Francke, U., Haynes, B. F., and Aruffo, A. (1995) *J. Exp. Med.* **181,** 2213–2220
16. Bodian, D. L., Skonier, J. E., Bowen, M. A., Neubauer, M., Siadak, A. W., Aruffo, A., and Bajorath, J. (1997) *Biochemistry* **36,** 2637–2641
17. Bowen, M. A., Bajorath, J., D'Egidio, M., Whitney, G. S., Palmer, D., Kobarg, J., Starling, G. C., Siadak, A. W., and Aruffo, A. (1997) *Eur. J. Immunol.* **27,** 1469–1478
18. Skonier, J. E., Bodian, D. L., Emswiler, J., Bowen, M. A., Aruffo, A., and Bajorath, J. (1997) *Protein Eng.* **10,** 943–947
19. Degen, W. G., Van Kempen, L. C. L. T., Gijzen, E. G., Van Groningen, J. J., Van Kooyk, Y., Bloemers, H. P. J., and Swart, G. W. M. (1998) *Am. J. Pathol.* **152,** 805–813
20. Van Kempen, L. C. L. T., Van den Oord, J., Van Muijen, G., Weidle, U. H., Bloemers, H. P. J., and Swart, G. W. M. (2000) *Am. J. Pathol.* **156,** 769–774
21. Nelissen, J. M., Peters, I. M., De Grooth, B. G., Van Kooyk, Y., and Figdor, C. G. (2000) *Mol. Biol. Cell.* **11,** 2057–2068
22. Feizi, T. (1994) *Trends Biochem. Sci*. **19**, 233–234
23. Silletti, S., Mei, F., Sheppard, D. and Montgomery, A. M. (2000) *J. Cell. Biol.* **149,** 1485–1502
24. Van Muijen, G. N., Cornelissen, L. M., Jansen, C. F., Figdor, C. G., Johnson, J. P., Brocker, E. B., and Ruiter, D. J. (1991) *Clin. Exp. Metastasis* **9,** 259–272
25. Bowen, M. A., Bajorath, J., Siadak, A. W., Modrell, B., Malacko, A. R., Marquardt, H., Nadler, S. G., and Aruffo, A. B. (1996) *J. Biol. Chem.* **271,** 17390–17396
26. Bowen, M. A., Aruffo, A. A., and Bajorath, J. (2000) *Proteins* **40**, 420–428
27. Kasper, C., Rasmussen, H., Kastrup, J. S., Ikemizu, S., Jones, E. Y., Berezin, V., Bock, E., and Larsen, I. (2000) *Nat. Struct. Biol.* **7,** 389–393
28. Aruffo, A., Bowen, M. A., Patel, D. D., Haynes, B. F., Starling, G. C., Gebe, J. A., and Bajorath, J. B. (1997) *Immunol. Today* **18,** 498–504

Molecular Basis for the Homophilic Activated Leukocyte Cell Adhesion Molecule (ALCAM)-ALCAM Interaction

Léon C. L. T. van Kempen, Judith M. D. T. Nelissen, Winfried G. J. Degen, Ruurd Torensma, Ulrich H. Weidle, Henri P. J. Bloemers, Carl G. Figdor and Guido W. M. Swart

J. Biol. Chem. 2001, 276:25783-25790.
doi: 10.1074/jbc.M011272200 originally published online April 16, 2001
